EUROPEAN COMMISSION
DIRECTORATE-GENERAL
Joint Research Centre

Institute for Environment and Sustainability

Medium Resolution Imaging Spectrometer (MERIS)

Level 2 Land Surface Products Algorithm Theoretical Basis Document

Nadine Gobron, Ophélie Aussedat, Bernard Pinty
Malcolm Taberner & Michel Verstraete

Institute for Environment and Sustainability
Joint Research Centre, TP 440
I–21020 Ispra (VA), Italy

| Revision 3.0, November 25, 2004

| **JRC Publication No. EUR 21387 EN**

Contents

List of Figures

List of Tables

1 Introduction

1.1 Purpose

This Algorithm Theoretical Basis Document (ATBD) describes an algorithm used to retrieve information on the nature and properties of vegetated terrestrial surfaces from an analysis of Level 1B data which are generated by the Medium Resolution Imaging Spectrometer (MERIS) of the European Space Agency (ESA).

The algorithm takes the form of a spectral index, *i.e.*, a set of formulae which transform calibrated spectral directional reflectances into a single numerical value. These formulae are designed to extract some information of interest from the measurements. The index described in this ATBD has been optimized to assess the presence on the ground of healthy live green vegetation. The optimization procedure has been constrained to provide an estimate of the Fraction of Absorbed Photosynthetically Active Radiation (FAPAR) in the plant canopy, although the index is expected to be used in a wide range of applications.

This algorithm delivers, in addition to the FAPAR product, the so-called rectified reflectance values in the red and near-infrared spectral bands. These are virtual reflectances largely decontaminated from atmospheric and angular effects which are still depending on the sensor and platform orbital specifications.

This document identifies the sources of input data, outlines the physical principles and mathematical background justifying this approach, describes the proposed algorithm, and lists the assumptions and limitations of this technique.

Polynomials coefficients values are updated and supersede those given in previous versions of ATBD.

1.2 Algorithm identification

The algorithm described below is called the MERIS Global Vegetation Index (MGVI). The corresponding module in the MERIS ground segment data flow is identified as TOAVI, and uses Top Of Atmosphere (TOA) Level 1B data as input and the rectified reflectances are noted rect rho.

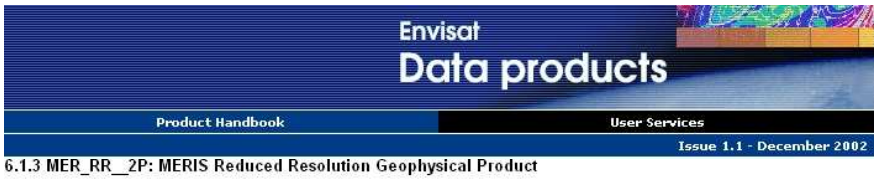

6.1.3 MER_RR__2P: MERIS Reduced Resolution Geophysical Product

Table 6.4

MER_RR__2P

MERIS Reduced Resolution Geophysical Product

File Structure

Data Sets 25

MPH 6.6.1.	Main Product Header
Chl_1, TOAVI - MDS(15) 6.6.118.	Level 2 MDS(15) algal index I TOAVI Cloud top pressure
YS, SPM, Rect. Rho- MDS(16) 6.6.119.	Level 2 MDS(16) yellow substance total suspended matter or rectified reflectances

Source: Envisat Handbook (c) ESA December 2002.

1.3 Scope

This document outlines the algorithm which is routinely applied by the ESA ground segment to generate both a FAPAR product, *i.e.*, the MERIS Global Vegetation Index (MGVI) and rectified red and near-infrared reflectance values.

1.4 Revision history

The previous version of this document, revision 2.0, was dated January 22, 2002.

The current version, version 3.0, includes the developments presented in Gobron et al. (2002) and supersedes all previous versions.

1.5 Other relevant documents

Other references to technical reports, ATBDs and additional information about MERIS can be found at the following address:
`http://envisat.estec.esa.nl/Satellite/instrument/MERIS/`. A series of relevant reports and articles are included in the bibliography list of this ATBD.

A package for the BEAM software is available and can be downloaded from the following ftp anonymous web. site: `ftp-gvm.jrc.it` in the directory `/gobrona/beam/mgvi/`

Validation exercices are on going since the launch on ENVISAT (see Gobron et al. (2002), Gobron et al. (2003) and Gobron et al. (2003))

A time compositing procedure suitable for a number of surface applications requiring good geographical coverage is described in Pinty et al. (2002).

2 Algorithm overview

2.1 Objectives of surface retrievals

The bulk of the solar radiation available to the Earth system is absorbed at or near the oceanic and continental surface. This energy is ultimately released to the atmosphere through the fluxes of infrared radiation, as well as sensible and latent heat. The phytosphere, which itself accounts for most of the biomass, affects these exchanges through a surface of contact (leaves) with the atmosphere estimated to be larger than the surface of the entire planet.

The state and evolution of terrestrial vegetation is characterized by a large number of physical, biochemical and physiological variables. Few of these are directly observable from space, but they jointly determine the Fraction of Absorbed Photosynthetically Active Radiation (FAPAR) which acts as an integrated indicator of the status and health of the plant canopy, and can reasonably be expected to be retrieved by remote sensing techniques. FAPAR plays a critical role in the biospheric path of the global carbon cycle and in the determination of the primary productivity of the phystosphere.

The state and evolution of the terrestrial vegetation cover thus concern a large number of users through such applications as agriculture, forestry, environmental monitoring, etc. Since plant canopies significantly affect the spectral and directional reflectance of solar radiation, it is expected that the analysis of repeated observations of these reflectances

may lead to a better understanding of the fundamental processes controlling the biosphere, which, in turn, will support the definition of sustainable policies of environmental exploitation, and the control of the effectiveness of any adopted rules and regulations.

The overall scientific objective of the MERIS Global Vegetation Index is to exploit the spectral reflectance measurements acquired by this instrument to provide users with reliable qualitative and quantitative information on the state of the plant cover over terrestrial areas. Specifically, the index value is meant to be easily interpreted in terms of FAPAR values.

The design of the MERIS Global Vegetation Index requires, in a first step, the estimate of the so-called rectified reflectances at the red and near-infrared wavelengths in order to minimize atmospheric and angular perturbations. These intermediary land surface products should prove useful for documenting the state of the land surfaces and also assessing the spatio-temporal variations in land cover type. Specifically, these rectified reflectances correspond to the amplitude parameter of the BRF entering the Rahman, Pinty, Verstraete (RPV) parametric model (Rahman et al. 1993). These are virtual, *i.e.*, not directly measurable in the field, spectral reflectances which are, at best, decontaminated from atmospheric and angular effects.

2.2 Instrument characteristics

The MERIS instrument has been described in a number of publications, such as MERIS Scientific Advisory Group (1995) and Rast et al. (1999). For the purpose of this document, it is sufficient to recall that MERIS is a programmable push-broom instrument acquiring multispectral measurements between 390 and 1040 nm, at a minimum usable resolution of 5 nm. Fifteen bands of programmable location and width can be downloaded simultaneously at the full resolution of approximately 300 m, at least for limited regions. Global coverage at a spatial resolution of 1.2 km will be operationally available on a daily basis. MERIS is not designed to acquire simultaneous measurements over any particular site under more than one geometry of illumination and observation, however, orbital constraints and instrumental specifications will inevitably result in different such geometries from pixel to pixel within a single image and for any given location between overpasses on consecutive days. The proposed algorithm will thus focus on the exploitation of the spectral variability of the data, keeping in mind the possible perturbing effects that may result from variations in geometry within and between successive images.

2.3 Retrieval strategy

Mathematical models implementing specific algorithms are essential to extract relevant, reliable and accurate information from remotely sensed data (Verstraete et al. 1996). Existing tools range from empirical approaches to physically based models. The latter provide, in principle, the most complete and reliable description of the target of interest, but this approach requires a rather detailed understanding of the various physical processes which affect the measurements. The inversion of these models against remote sensing data necessitates significant computing resources. The systematic application of these techniques in the analysis of MERIS data alone is not appropriate because of the insufficient angular sampling of this sensor.

More empirical (but much simpler) approaches have been suggested and extensively used over the past decades to attempt to retrieve the essence of the desired information at the cost of substantial assumptions on the observed media. Physical effects typically not accounted for include the anisotropy of land surfaces, the architecture of the vegetation, the optical thickness of the atmosphere, and the type of aerosol. Among these empirical approaches, vegetation indices, or more generally spectral indices, have been shown to be convenient tools to monitor the broad spatial characteristics of the landscape and their temporal evolution. These tools focus exclusively on the interpretation of the spectral signature of the various objects that interact with the incoming solar radiation. In particular, they exploit the fact that live green vegetation strongly absorbs solar radiation in the red spectral band, and strongly scatters radiation in the near-infrared band.

The scientific objective of the proposed algorithm is thus to deliver a spectral index optimized for the analysis of MERIS data with the following design requirements:

1. Over areas deemed to be at least partially vegetated, the index should be sensitive to the amount of live green vegetation at the surface, and specifically provide an estimate of the FAPAR in the observed canopies, irrespective of the soil and atmospheric conditions that may prevail, or the illumination and observation geometries.

2. to offer excellent discrimination capabilities, *i.e.*, the opportunity to distinguish various target types.

3. The performance of the index should be independent of the spatial resolution.

4. The actual estimation of the numerical value of the index should require minimal computional costs. This is deemed to mean that the computation of the index is expected to be made on a pixel-by-pixel basis but should require less than 1000 arithmetic (floating point) operations.

5. The index should directly exploit Level 1B MERIS data, *i.e.*, top-of-atmosphere reflectance factors in no more than 8 spectral bands.

3 Algorithm description

3.1 Physics of the problem

As MERIS is a monodirectional spectral imaging instrument, the proposed algorithm must rely exclusively on the spectral signature of the observed targets to retrieve the desired information.

The general theory behind the design of optimal spectral indices has been described in Verstraete and Pinty (1996), and its specific application to the MERIS instrument has been addressed in Govaerts et al. (1999), Gobron et al. (1999) and Gobron et al. (2000). The most recent implementation of the algorithm assumes that, 1) the FAPAR can be used to quantify the presence of vegetation and, 2) radiation transfer model simulations can be used to define appropriate scenarios in the absence of MERIS-like data sets over different representative land surfaces.

The bulk of the information on the presence of vegetation is contained *a priori* in the red and the near-infrared spectral bands, typically at wavelengths such as 681 and

865 nm. Addressing the atmospheric problem consists in converting Top Of Atmosphere (TOA) Bidirectional Reflectance Factors (BRFs) into Top Of Canopy (TOC) BRFs.

Two classes of atmospheric radiative processes affect the measurements made by spaceborne satellites: absorption and scattering. Absorption of radiation by specific gases can be largely avoided by carefully choosing the spectral location of narrow bands. Further corrections can be implemented, if needed, by estimating the amount of these gases from other spectral bands. The effect of scattering cannot be avoided, and both molecular and aerosol scattering are strongly dependent on the wavelength of radiation. Hence, measurements in the blue region of the solar spectrum will provide values much more sensitive to atmospheric scattering than at longer wavelengths. In this approach, the characterization of plant canopies over fully or partially vegetated pixels currently relies on the analysis of data in 3 MERIS spectral bands, namely 442, 681, and 865 nm.

The design of an optimal spectral index relies on the availability of actual or simulated measurements, together with detailed documentation of the physical processes which controlled these observations. In the absence of actual MERIS data, a coupled surface-atmosphere model has been used to generate realistic MERIS measurements. A LookUp Table (LUT) of bidirectional reflectance factors representing the MERIS-like data has been created using the physically-based semidiscrete model of Gobron et al. (1997) to represent the spectral and directional reflectance of horizontally homogeneous plant canopies, as well as to compute the values of FAPAR in each of them. The soil data required to specify the lower boundary condition in this model were taken from Price (1995). The spectral values for the leaf reflectance and transmittance were simulated using the model from Jacquemoud and Baret (1990). The 6S atmospheric model of Vermote et al. (1997) has been used to represent the atmospheric absorption and scattering effects on the measured reflectances. The FAPAR values are computed using the closure of the energy balance inside the plant canopy in the spectral range 400 to 700 nm. The various geophysical scenarios performed to simulate the radiance fields are summarized in Table 1 and the geometrical conditions of illumination and observation are given in Table 2. The sampling of the vegetation parameters and angular values were chosen to cover a wide range of environmental conditions. These simulations constitute the basic information used to optimize the vegetation index. The sampling selected to generate the LUT has been chosen so as to generate a robust global vegetation index.

Once this LUT has been created, the design of an optimal spectral index consists in defining the mathematical combination of spectral bands which will best account for the variations of the variable of interest (here, FAPAR) on the basis of (simulated) measurements, while minimizing the effect of perturbing factors such as atmospheric or angular effects. This process is described in the next section.

3.2 Mathematical description of the algorithm

The proposed algorithm to compute MGVI and associated products is organized around three main steps:

1. As mentioned previously, because of the sampling implemented by the MERIS instrument in the angular domain, it is not possible to retrieve the anisotropy of the radiance field. A parametric anisotropic function is thus implemented to account for variations in the signal due to changes in the geometrical conditions. The bidirec-

Table 1: Geophysical scenarios used to simulate the radiance fields.

Medium	**Variable**	**Meaning**	**Range of values**
Atmosphere model (Vermote *et al.*, 1997)	τ_s	Aerosol opt. thickness	0.05, 0.3 and 0.8
Vegetation model (Gobron *et al.*, 1997)	LAI	Leaf Area Index	0, 0.5, 1, 2, 3, 4, and 5
	H_c	Height of Canopy	0.5 and 2 m
	d_ℓ	Equivalent $\emptyset$ of single leaf	0.01 and 0.05 m
	LAD	Leaf Angle Distribution	Erectophile, Planophile
Soil data base (Price, 1995)	r_s	Soil reflectance	5 soil spectra, from dark to bright

Table 2: Illumination and observation geometries used to simulate the radiances fields.

Variable	**Angle**	**Values**
θ_0	Solar zenith angle	20 and 50°
θ_v	Satellite zenith angle	0, 25 and 40°
ϕ	Sun-Satellite relative azimuth	0, 90 and 180°

tional reflectance model of Rahman et al. (1993) (RPV) is assumed to be appropriate for this task:

$$\rho_i(\theta_0, \theta_v, \phi) = \rho_{i0}\, F(\theta_0, \theta_v, \phi; k_i, \Theta_i^{hg}, \rho_{ic}) \tag{1}$$

where F characterizes the anisotropy of the medium in terms of three unknown parameters, namely k_i, Θ_i^{hg} and ρ_{ic} which depends exclusively on the intrinsic properties of the type of the geophysical system for a given spectral band i. The function $F(\Omega; k_i, \Theta_i^{hg}, \rho_{ic})$ with $\Omega = (\theta_0, \theta_v, \phi)$ is given by

$$F(\Omega; k_i, \Theta_i^{hg}, \rho_{ic}) = f_1(\theta_0, \theta_v, k_i)\, f_2(\Omega, \Theta_i^{hg})\, f_3(\Omega, \rho_{ic}) \tag{2}$$

where

$$f_1(\theta_0, \theta_v, k_i) = \frac{(\cos\theta_0\, \cos\theta_v)^{k_i - 1}}{(\cos\theta_0 + \cos\theta_v)^{1-k_i}} \tag{3}$$

$$f_2(\Omega, \Theta_i^{hg}) = \frac{1 - {\Theta_i^{hg}}^2}{\left(1 + 2\,\Theta_i^{hg}\, \cos g + {\Theta_i^{hg}}^2\right)^{3/2}} \tag{4}$$

$$f_3(\Omega, \rho_{ic}) = 1 + \frac{1 - \rho_{ic}}{1 + G} \tag{5}$$

with

$$G = \left(\tan^2\theta_0 + \tan^2\theta_v - 2\,\tan\theta_0\,\tan\theta_v\,\cos\phi\right)^{1/2} \tag{6}$$

$$\cos g = \cos\theta_0\,\cos\theta_v + \sin\theta_0\,\sin\theta_v\cos\phi \tag{7}$$

The characterization of a geophysical system with the RPV model requires an estimate of four parameter values, namely ρ_{i0}, k_i, Θ_i^{hg} and ρ_{ic}, which are independent of the geometry of illumination and observation Ω.

The parameters required by the function F are optimized separately in each of the three bands, using the simulated BRFs emerging at the top of atmosphere.

2. The MERIS data acquired in the blue (band 2 at 442 nm) is combined with those from the red (band 8 at 681 nm) and near-infrared (band 13 at 865 nm) regions traditionally used to monitor vegetation, in order to generate "rectified bands" at these latter two wavelengths. This "rectification" is done in such a way as to minimize the difference between the rectified bands and the spectral reflectances that would have been measured at the top of the canopy under identical geometrical conditions but in the absence of the atmosphere.

3. The spectral index, MGVI, is then generated on the basis of these "rectified bands".

The proposed algorithm assumes that ratios of polynomials are appropriate to generate the rectified red band reflectances ($n = 1$), the rectified near-infrared band reflectances ($n = 2$) and the final formulae representing the FAPAR axis ($n = 0$):

$$g_n(B_1, B_2) = \frac{l_{n,1}B_1^2 + l_{n,2}B_2^2 + l_{n,3}B_1B_2 + l_{n,4}B_1 + l_{n,5}B_2 + l_{n,6}}{l_{n,7}B_1^2 + l_{n,8}B_2^2 + l_{n,9}B_1B_2 + l_{n,10}B_1 + l_{n,11}B_2 + l_{n,12}} \tag{8}$$

where B_1 and B_2 are the spectral bands at the appropriate step. The desired MERIS vegetation index is given by:

$$\mathrm{MGVI} = g_0(\rho_{R681}, \rho_{R865}) \tag{9}$$

where ρ_{R681} and ρ_{R865} are the rectified reflectance values in the red and near-infrared bands described above. These, in turn, are estimated with

$$\rho_{R681} = g_1(\tilde{\rho}_{442}, \tilde{\rho}_{681}) \tag{10}$$

$$\rho_{R865} = g_2(\tilde{\rho}_{442}, \tilde{\rho}_{865}) \tag{11}$$

where

$$\tilde{\rho}_i = \frac{\rho_i^*(\theta_0, \theta_v, \phi)}{F(\theta_0, \theta_v, \phi; k_i, \Theta_i^{hg}, \rho_{ic})} \tag{12}$$

and where ρ_i^* denotes the (simulated) top of atmosphere bidirectional reflectance factor in band i, while $\tilde{\rho}_i$ is the bidirectional reflectance factor normalized by the anisotropic function F. An optimization procedure is applied to retrieve successively the optimal values of the coefficients intervening in the three steps mentioned above, namely k_i, Θ_i^{hg} and ρ_{ic}, and $l_{n,j}$ for the polynomials g_n, both for the rectified bands and for the final index itself.

1. In the first step, it is assumed that the anisotropic shapes of the BRFs simulated at the top of the atmosphere may change with the spectral wavelength of interest, but do not depend on the geophysical systems specified to generate the BRFs. Accordingly, for a given spectral band, the three parameters of the anisotropic function F

are forced to be constant over the entire set of geophysical scenarios considered. In practice, this condition is achieved by minimizing the following cost functions:

$$\delta_i^2 = \sum_{\zeta,\Omega} \left[\left(\frac{\rho_i^*(\Omega)}{F(\Omega; k_i, \Theta_i^{hg}, \rho_{ic})} \right) - \tilde{\rho}_i \right]^2 \rightarrow 0 \tag{13}$$

where ζ represents the geophysical domain and Ω the angular domain over which the optimization is sought.

Since $\tilde{\rho}_i$ is assumed to be constant in the RPV model for each individual geophysical system taken separately, we can estimate the mean value of the BRFs over the Ω space for every geophysical system:

$$\frac{1}{N_{obs}} \sum_{\Omega} \rho_i^*(\Omega_j) = \frac{1}{N_{obs}} \sum_{\Omega} \tilde{\rho}_i \times F(\Omega_j; k_i, \Theta_i^{hg}, \rho_{ic}) \tag{14}$$

$$= \tilde{\rho}_i \frac{1}{N_{obs}} \sum_{\Omega} F(\Omega_j; k_i, \Theta_i^{hg}, \rho_{ic}) \tag{15}$$

where N_{obs} is the total number of angular situations. The model coefficient $\tilde{\rho}_i$ is thus approximated for each geophysical system as

$$\tilde{\rho}_i = \frac{1}{N_{obs}} \sum_{\Omega} \rho_i^*(\Omega_j) \Big/ \frac{1}{N_{obs}} \sum_{\Omega} F(\Omega_j; k_i, \Theta_i^{hg}, \rho_{ic}) \tag{16}$$

The cost function is rewritten as follows:

$$\delta_i^2 = \sum_{\zeta} \left[\frac{\rho_i^*(\Omega)}{F(\Omega; k_i, \Theta_i^{hg}, \rho_{ic})} \frac{1}{N_{obs}} \sum_{\Omega} F(\Omega_j; k_i, \Theta_i^{hg}, \rho_{ic}) - \frac{1}{N_{obs}} \sum_{\Omega} \rho_i^*(\Omega_j) \right]^2 \rightarrow 0 \tag{17}$$

2. To satisfy the various requirements described above, the optimization procedure is applied in the 681 nm and 865 nm bands separately, to derive the coefficients of g_1 and g_2. This is achieved by minimizing the following cost functions:

$$\delta_{g_i}^2 = \sum_{\zeta} \left[g_i(\tilde{\rho}_{442}, \tilde{\rho}_i) - \tilde{\rho}_i^{TOC} \right]^2 \rightarrow 0. \tag{18}$$

where

$$\tilde{\rho}_i^{TOC} = \frac{\rho_i^{TOC}(\Omega)}{F(\Omega, k_i^{TOC}, \Theta_i^{hg,TOC}, \rho_{ic}^{TOC})} \tag{19}$$

for which the anisotropic parameters, namely $k_i^{TOC}, \Theta_i^{hg,TOC}, \rho_{ic}^{TOC}$, were previously optimized at the top of canopy level.

3. Following the rectification of the BRFs in the previous step, the coefficients of g_0 are evaluated by minimizing the following cost function:

$$\delta_{g_0}^2 = \sum_{\zeta} \left[g_0(\rho_{R681}, \rho_{R865}) - \text{FAPAR} \right]^2 \rightarrow 0. \tag{20}$$

In other words, the MGVI is forced to take on values as close as possible to the FAPAR associated with the specified plant canopy scenarios. The simulated top-of-atmosphere spectral and directional reflectances generated by the coupled model have been exploited with an extended version of the FACOSI tool (Govaerts et al. 1999) to adjust the MGVI on the basis of the given set of equations. The numerical results are summarized in Tables 3 to 6.

Table 3: **NEW** Values of the parameters for the anisotropic function F.

band	**Parameter values**		
	ρ_{ic}	k_i	Θ_i^{hg}
442 nm	0.24012	0.56192	−0.04203
681 nm	−0.46273	0.70879	0.037
865 nm	0.63841	0.86523	−0.00123

Table 4: **NEW** Coefficients for the polynomial g_1.

$l_{1,1}$	$l_{1,2}$	$l_{1,3}$	$l_{1,4}$	$l_{1,5}$	$l_{1,6}$
−9.26150	3.2545	9.8268	0.537371	0.363495	0.00235
$l_{1,7}$	$l_{1,8}$	$l_{1,9}$	$l_{1,10}$	$l_{1,11}$	$l_{1,12}$
0	0	0	0	0	1.0

Table 5: **NEW** Coefficients for the polynomial g_2.

$l_{2,1}$	$l_{2,2}$	$l_{2,3}$	$l_{2,4}$	$l_{2,5}$	$l_{2,6}$
−0.47131	−0.0451590	−0.807070	0.198120	−0.00690978	−0.0210847
$l_{2,7}$	$l_{2,8}$	$l_{2,9}$	$l_{2,10}$	$l_{2,11}$	$l_{2,12}$
−0.0483620	−0.545070	−1.10270	0.120625	0.518928	−0.198726

Table 6: **NEW** Coefficients for the polynomial g_0.

$l_{0,1}$	$l_{0,2}$	$l_{0,3}$	$l_{0,4}$	$l_{0,5}$	$l_{0,6}$
0.0	0.0	0.0	−0.306	0.255	0.0045
$l_{0,7}$	$l_{0,8}$	$l_{0,9}$	$l_{0,10}$	$l_{0,11}$	$l_{0,12}$
1.0	1.0	0.0	0.64	−0.64	0.1998

Figures (1) and (2) illustrate the impact of the "rectification" procedure, which combines TOA reflectances in the 442 nm band with TOA reflectances in the 681 nm and 865 nm bands, respectively. The left panels on these figures show the relationships between the spectral BRFs TOC normalized by the anisotropic function F, and BRFs TOA for all geophysical and angular scenarios described in Table 1. The scattering of the points is caused by changes in the atmospheric conditions and by the relative geometry of illumination and observation. The right panels show the effect of the "rectification" process, which reduces this dispersion. A perfect "rectification" would collapse all points on the 1:1 line for each of the surface types considered. It can be seen that this process is particularly efficient over dense vegetation, and that it reduces the systematic bias due to atmospheric effects on BRFs in both bands.

Figure (3) provides information on the performance of MGVI. The right panel shows the isolines of the MGVI in the spectral space of the rectified bands at 681 nm and 865 nm.

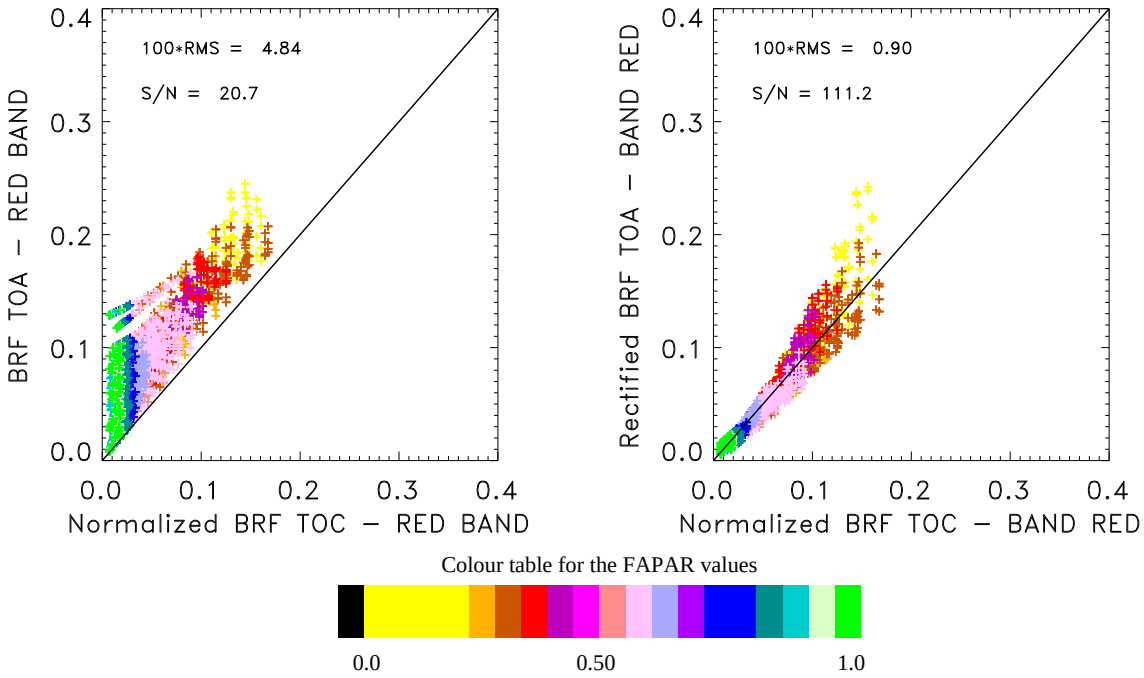

Figure 1: **NEW** Left panel: relationship between the BRFs TOC normalized by the anisotropic function F, and BRFs TOA, for all conditions given in Table 1, in the 681 nm band. Right panel: relationship between the "rectified" reflectances and the corresponding BRFs TOC normalized by the anisotropic function F. The various colours represent different values of FAPAR for the plant canopies described in Table 1.

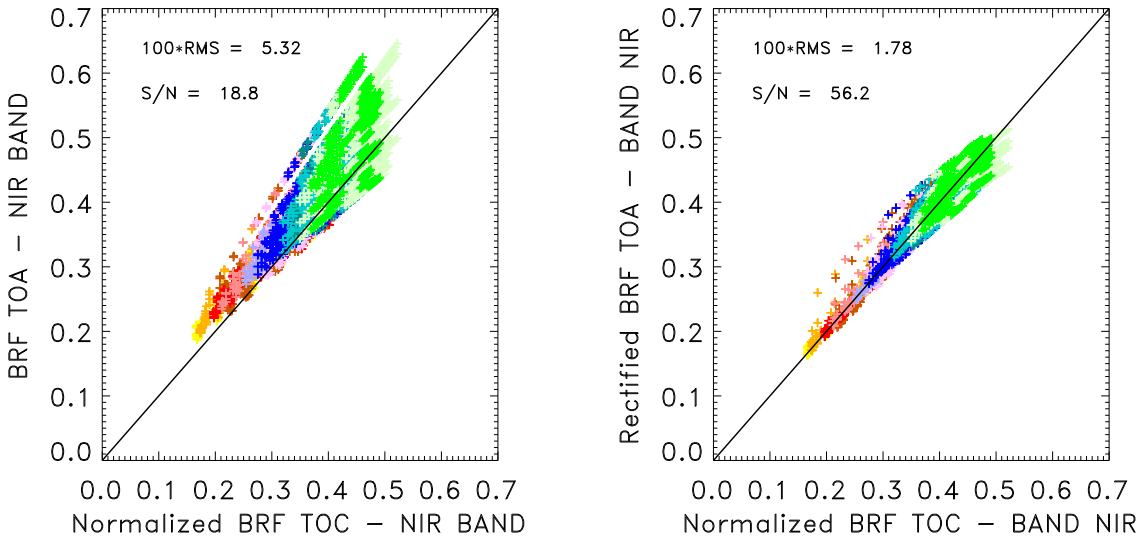

Figure 2: **NEW** Same as Figure (1) except for the 865 nm band.

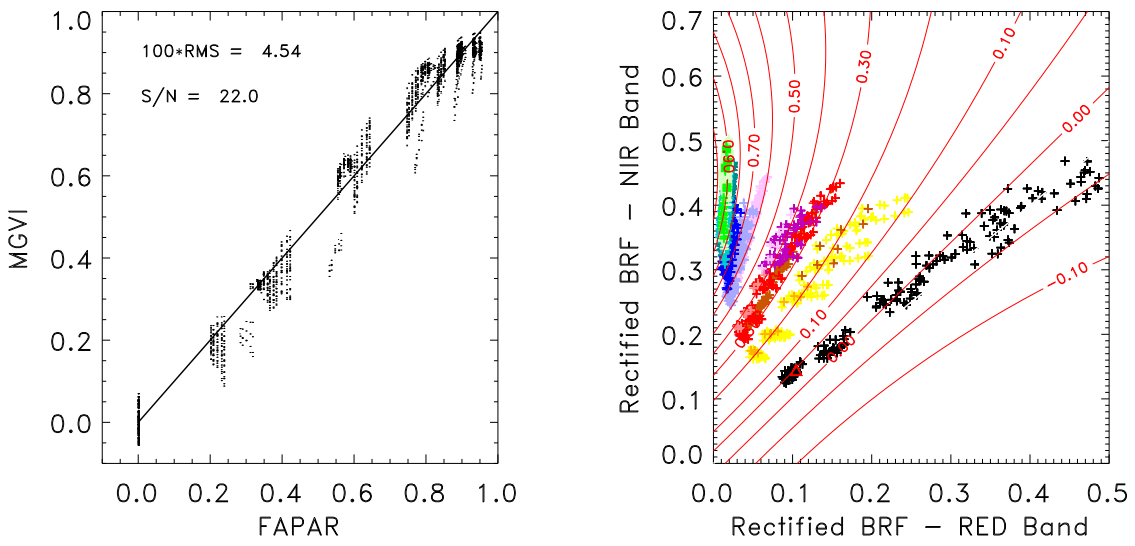

Figure 3: **NEW** The right panel shows the isolines of MGVI in the rectified (681 nm, 865 nm) spectral space together with the simulated radiances at the top of the atmosphere (see Table 1). The left panel shows the relationship between the index and the FAPAR values.

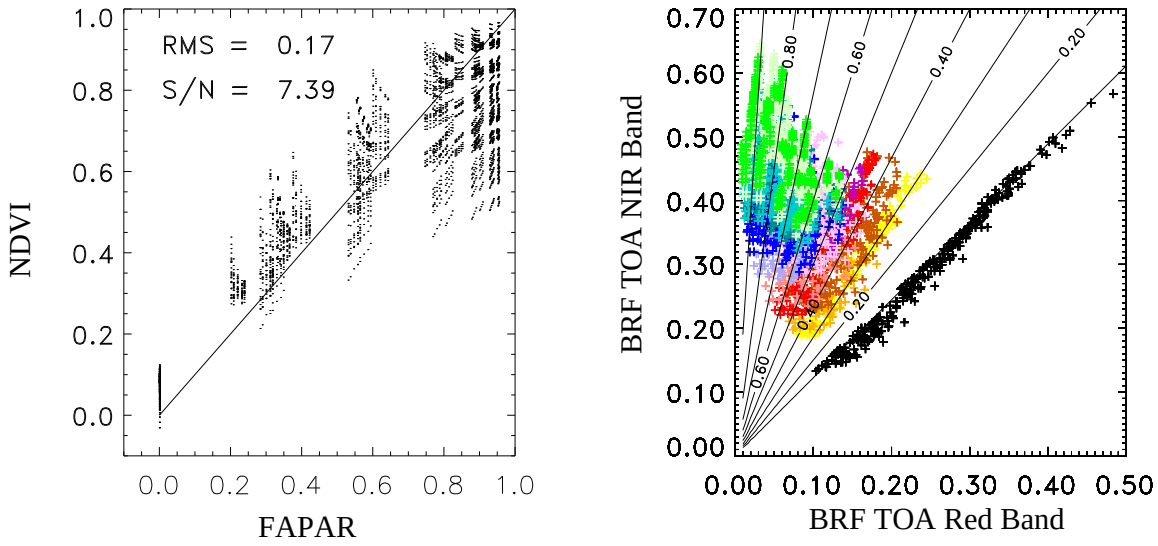

Figure 4: The right panel shows the isolines of NDVI in the (681 nm, 865 nm) spectral space together with the simulated radiances at the top of the atmosphere (see Table 1). The left panel shows the relationship between the index and the FAPAR values.

It can be seen that the MGVI varies between 0 and 1 over partially and fully vegetated surfaces and takes negative values out of the spectral domain of interest. The left panel of the same figure shows that the MGVI is close to the FAPAR with a root mean square deviation equal to 0.05. Most of the remaining variability between FAPAR and MGVI is probably caused by the various conditions that were considered in the geophysical scenarios (see Table 1). In fact, this variability results from conflicting requirements on the insensitivity of the MGVI to soil, atmospheric and geometrical effects in the MERIS spectral bands.

3.3 Error budget estimates

Since the MGVI has been optimized to provide a high sensitivity to FAPAR, a measurable biophysical variable, its capacity to detect the presence of green vegetation can be objectively assessed. For the particular geophysical scenarios in Table 1 and angular sampling given in Table 2, the root mean square deviation value of the fit between these two quantities is 0.05. Following the method proposed by Leprieur et al. (1994), the performance of MGVI can be evaluated with the help of a signal to noise ratio. In the present case, it was found that the signal to noise ratio of the MGVI is equal to 22.00. By comparison, the widely used Normalized Difference Vegetation Index (NDVI), computed on the basis of bands at 681 nm and 865 nm exhibits a non-linear relationship with respect to FAPAR variations and the corresponding signal to noise ratio is only 7.39 (see Figure 4).

3.4 Practical considerations

3.4.1 Quality control and diagnostics

Two 1-bit flags have been assigned to the MGVI algorithm. The default values of both flags is 0, which represents nominal or acceptable conditions. The following describes error or exception conditions, which are flagged by setting the corresponding bit to 1. These tests are necessary for the proper computation of the MGVI product:

1. It is assumed that no processing occurs if any of the 3 spectral bands used by this algorithm is saturated, or missing, for the current pixel.

2. It is assumed that mathematical errors such as numerical overflow, underflow, or division by zero, are caught.

3. If the calibrated reflectance at the following three spectral bands: 442, 681, and 865 nm are greater than: 0.3, 0.5 and 0.7, respectively, then the MGVI is not computed and this situation is flagged.

4. If the calibrated reflectance of the 865 nm spectral band is less than 1.25× that of the calibrated reflectance of the 681 nm spectral band, then the MGVI is not computed and this situation is flagged. ($i.e., \rho^*_{865}(\theta_s, \theta_v, \phi) < 1.25 \times \rho^*_{68}(\theta_s, \theta_v, \phi)$)

5. If either of the two rectified bands, ρ_{R865} or ρ_{R681}, computed from equations (10) and (11), respectively, goes negative, then this circumstance is flagged and MGVI not calculated.

In the allocated 2 flag system, items 2, 3 and 4 can be allocated to a single flag value `FLAG1` and item 5 to `FLAG2`.

See section 4.2 for further information on possible future improvements of this flag system.

3.4.2 Output

Allocation restrictions mean that the output generated by this algorithm consists in one index value for the MGVI, one for the rectified red, and one for the rectified near infrared, and two single bit flags, labelled `FLAG1` and `FLAG2`, for each pixel in the Level 1B data input stream. The MGVI product and the rectified bands are packed in 8 bit unsigned chars.

The quality tests are described in section 3.4.1. If either of the flags `FLAG1` or `FLAG2` are set to 1, the value of MGVI is not computed and the reported value is set to an error value.

If both flags are set to 0 and if the value of MGVI is less than 0, the reported value of MGVI is set to 0.

If both flags are set to 0 and if the value of MGVI is greater than 1, the reported value of MGVI is set to 1.

Whenever both quality flags are set to 0, the value of MGVI is computed and reported. In this case, the index value is coded on 8 bits, from 0 to 250, offering 250 different values of FAPAR within the range $[0, 1]$, with a step of $4.0\,10^{-3}$.

4 Assumptions and limitations

4.1 Assumptions

The following assumptions have been made in the design of the MERIS Global Vegetation Index (MGVI):

1. Non-saturating MERIS Level 1B calibrated reflectances will be available in the following 3 spectral bands: 442, 681, and 865 nm.
2. The level 1B spectral reflectances used as input to this algorithm will have been identified as corresponding to land surface pixels.
3. The Level 1B spectral reflectances used as input to this algorithm will have been corrected for the seasonally variable distance between the Earth and the Sun.
4. The plane-parallel approximation for radiation transfer has been assumed to be valid in the atmosphere.
5. Plant canopies are assumed to be horizontally homogeneous within the MERIS pixel.
6. All orographic effects have been ignored.
7. Adjacency effects have been ignored.
8. Substantial atmospheric aerosol loads, as observed in dust storms and heavily polluted areas are assumed to be screened out or sufficiently infrequent to not affect the global applicability of the algorithm.

4.2 Limitations

The following limitations apply to the algorithm described in this version of the document:

1. The retrieval of vegetation characteristics in hilly or mountainous regions may or may not be reliable. This question will have to be investigated after launch once actual MERIS data has become available over such regions. If the approach turns out to be unreliable in the presence of significant topographical features, additional tests may have to be implemented to screen out these regions on the basis of appropriate DEM data. This would imply access to the corresponding elevation data sets, to reliably navigated MERIS data, and the presence of an additional orographic flag.

2. The optimization of the MGVI was performed using a set of simulated TOA reflectance values which are expected to represent the most commonly encountered geophysical conditions. Although a wide range of possibilities were investigated, there is no guarantee that the most common geophysical scenarios (which are unknown at this time) have been implemented. If this is not the case, this may result in a systematic bias in the relationship between the MGVI and the FAPAR, but this situation can be corrected after launch with the help of appropriate field campaign measurements.

3. Currently, the rectified bands are produced using the MGVI logic, it is possible that these products contain significant information outwith the MGVI products. If this turns out to be the case, then different logic is likely to be required, in the commisioning phase, to extend the rectified domain.

5 Algorithm requirements

Three different ingredients are thus required to estimate MGVI: a data set of calibrated reflectances; a series of appropriate coefficients; and a set of mathematical functions. The calibrated reflectances are the BRFs measured by the MERIS instrument in the blue (band 2 at 442 nm), red (band 8 at 681 nm) and near-infrared (band 13 at 865 nm) spectral regions, together with the geometrical conditions of illumination and observation, namely θ_0, θ_v, and ϕ. The sun-sensor relative azimuth, ϕ, is limited to the range [0°, 180°] and the backscatter/hot spot (forwardscatter/specular) direction is defined at 0° (180°). The coefficients are those provided in Tables 3, 4, 5 and 6, and the mathematical functions are given by equations (2), (8), and (12).

References

Gobron, N., F. Mélin, B. Pinty, M. Taberner, and M. M. Verstraete (2003). Meris global vegetation index: Evaluation and performance. In *Proceedings of the MERIS User Workshop, Frascati, Italy, 10-14 November*, Volume SP 549, pp. pp 15. European Space Agengy.

Gobron, N., B. Pinty, M. M. Verstraete, and Y. Govaerts (1997). A semi-discrete model for the scattering of light by vegetation. *Journal of Geophysical Research 102*, 9431–9446.

Gobron, N., B. Pinty, M. M. Verstraete, and Y. Govaerts (1999). The MERIS Global Vegetation Index (MGVI): description and preliminary application. *International Journal of Remote Sensing 20*, 1917–1927.

Gobron, N., B. Pinty, M. M. Verstraete, and J.-L. Widlowski (2000). Advanced spectral algorithm and new vegetation indices optimized for up coming sensors: Development, accuracy and applications. *IEEE Transactions on Geoscience and Remote Sensing 38*, 2489–2505.

Gobron, N., M. Taberner, B. Pinty, F. Mélin, M. Verstraete, and J.-L. Widlowski (2002). Meris land algorithm: preliminary results. In *Proceedings of the ENVISAT Validation Workshop*, Volume SP 531, pp. pp. 10. European Space Agengy.

Gobron, N., M. Taberner, B. Pinty, F. Mélin, and M. M. Verstraete (2003). Meris global vegetation index: Evaluation and performance. In *Proceedings of the MERIS and ATSR Calibration and Geophysical Validation (MAVT), Frascati, Italy, 20-23 October, 2003*, Volume SP 541, pp. pp 15. European Space Agengy.

Govaerts, Y., M. M. Verstraete, B. Pinty, and N. Gobron (1999). Designing optimal spectral indices: a feasibility and proof of concept study. *International Journal of Remote Sensing 20*, 1853–1873.

Jacquemoud, S. and F. Baret (1990). PROSPECT: A model of leaf optical properties spectra. *Remote Sensing of Environment 34*, 75–91.

Leprieur, C., M. M. Verstraete, and B. Pinty (1994). Evaluation of the performance of various vegetation indices to retrieve vegetation cover from AVHRR data. *Remote Sensing Reviews 10*, 265–284.

MERIS Scientific Advisory Group (1995). MERIS: The Medium Resolution Imaging Spectrometer. Technical Report SP–1184, European Space Agency, Noordwijk.

Pinty, B., N. Gobron, F. Mélin, and M. M. Verstraete (2002). A Time Composite Algorithm Theoretical Basis Document. EUR Report No. 20150 EN, Joint Research Centre, Institute for Environment and Sustainability.

Price, J. C. (1995). Examples of high resolution visible to near-infrared reflectance spectra and a standardized collection for remote sensing studies. *International Journal of Remote Sensing 16*, 993–1000.

Rahman, H., B. Pinty, and M. M. Verstraete (1993). Coupled surface-atmosphere reflectance (CSAR) model. 2. Semiempirical surface model usable with NOAA Advanced Very High Resolution Radiometer data. *Journal of Geophysical Research 98*, 20,791–20,801.

Rast, M., J.-L. Bézy, and S. Bruzzi (1999). The ESA Medium Resolution Imaging Spectrometer MERIS -a review of the instrument and its mission. *International Journal of Remote Sensing 20*, (1682–1701).

Vermote, E., D. Tanré, J. L. Deuzé, M. Herman, and J. J. Morcrette (1997). Second simulation of the satellite signal in the solar spectrum: An overview. *IEEE Trans. Geoscience Remote Sensing 35-3*, 675–686.

Verstraete, M. M. and B. Pinty (1996). Designing optimal spectral indices for remote sensing applications. *IEEE Transactions on Geoscience and Remote Sensing 34*, 1254–1265.

Verstraete, M. M., B. Pinty, and R. B. Myneni (1996). Potential and limitations of information extraction on the terrestrial biosphere from satellite remote sensing. *Remote Sensing of Environment 58*, 201–214.

ISBN 92-894-8445-4